Capacitive Interdigital Sensors for Flexible Enclosures and Wearables

Mike Teodorescu [a,b]
[a] Information Systems Department, Boston College
[b] Research Affiliate, D-Lab, Massachusetts Institute of Technology
Cambridge, Massachusetts, USA
Mike.Teodorescu@bc.edu, hmteodor@mit.edu

Horia-Nicolai Teodorescu [a,b]
[a] Lab. BME, 'Gh. Asachi' Technical University of Iasi
[b] Institute of Computer Science of the Romanian Academy
Iasi, Romania
hteodor@etti.tuiasi.ro

***Abstract* – Recent applications related to flexible deployable enclosures for surgery and health care and to wearables may make use of capacitive sensors for monitoring the inflation state of the enclosure, the movements of the human body, and the detection of movements induced by respiration and heart activity (ballistocardiography). We propose the use of flexible, interdigital capacitive sensors in portable enclosures for medical applications, analyze the principles of operation of several versions of such sensors, and provide a theoretical foundation to their design and use, including limitations and errors. The paper also contributes to the analytic description of operation of flexible interdigital sensors, a topic not fully examined previously in the literature.**

Keywords-capacitive sensors; flexible sensor; sensor characteristics; theoretical analysis; movement sensor; ballistocardiography; flexible enclosure; wearable; medical applications.

I. Introduction

There is an increasing interest today in wearable and IoT connected sensors and systems. Such sensors could have a multitude of applications in manufacturing, entertainment and medicine. One type of sensor widely used is the capacitive one. Numerous applications of wearable, including textile capacitive sensors have been reviewed in several papers such as [1], [2], and [3]. Among the most popular applications are those for detecting touching and gripping, human body posture, 3D gesture sensing, indoor localization, biometric sensing, and medical applications [1], [4]. Numerous medical and health-related applications have been proposed for wearable capacitive sensors, including tremor assessment [5], [6], relative movements of body parts [5], [1], respiration, and ballistocardiography [7]. In many of these applications, the signal is sent to a computer by radio waves or IR, or IoT means are used to connect to larger networks [8].

During the last two decades, several flexible, portable enclosures for various applications, including medical ones, have been proposed [9], [10]. However, flexible capacitive sensors mounted on flexible walls have not been analyzed. We suggest the use of capacitive flexible sensors attached to or embedded in the walls of such enclosures for monitoring various ambient and biologic signals, moreover for monitoring the state of inflation of the collapsible enclosure. For such applications, small integrated capacitive sensors are of little use; instead, capacitive sensors covering large surfaces of the wall of the enclosure are needed. We focus on interdigital capacitive sensors in this paper. We provide theoretical foundations for the use of these sensors in the envisaged applications and determine their limitations and errors, thus providing a foundation for their use. We approach theoretically the operation of the discussed sensors because, while simulation methods can produce more detailed and precise results for specific cases of interdigital sensors with precise dimensions, the analytic approach helps the designer to gain a broad understanding.

II. Study Motivation

Interdigital capacitive sensors have been studied especially for macro- and microelectronic sensors and for MEMS applications and using simulation software [11-13], but much less for large and flexible devices and not theoretically for flexible sensors. Uncertainties in the operation of large surface sensors sewn, painted on, or embedded in the textiles may hamper their use and may pose the question of unquantifiable precision issues; these uncertainties may question the sensors' usability in medical applications. To remove this barrier, we present a detailed analysis of several errors and show a way of taking them into account. We apply the results to systems based on flexible enclosures. One such enclosure designed for surgery [14-16] is pictured in Fig. 1.

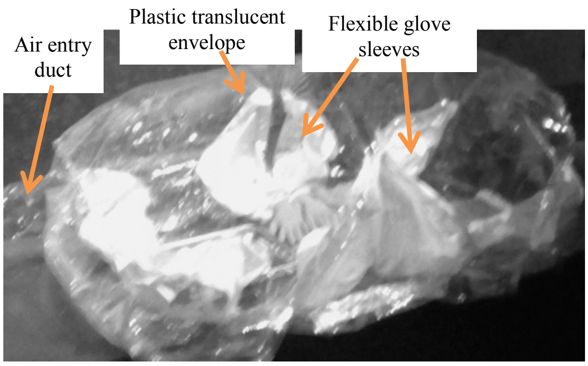

Figure 1. Example of a view of a portable, flexible enclosure proposed for surgery. Picture by HNT made in Design Museum exhibition London with Beazley Design of the Year Nominees for 2018, U.K., 15-17 Sep 2018. Design by SurgiBox Inc., US. Picture © 2018 HNT.

ISBN 978-80-261-0892-4, © University of West Bohemia, 2020

The enclosure in Fig. 1 is made of thin plastic film and has several surgical gloves and ports. See other pictures and a description in [17], p. 192. This type of enclosure easily accommodates flexible capacitive sensors on its lateral and bottom walls for patient movement sensing, as suggested in Fig. 2, as well as on the lateral walls and on the air duct, for assessing the smoothness of the walls.

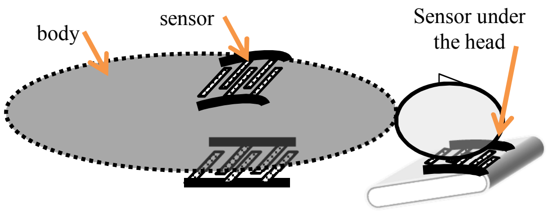

Figure 2. Example of several interdigital capacitive sensors positioning under the torso and under the head, for position and movement sensing, and on the torso (patch) for respiratory and ballistocardiographic signals). All sensors should be flexible.

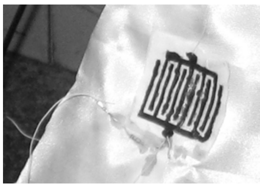

Figure 3. Example of interdigital capacitive sensor hand-painted on textile, identical with one used in [5].

An example of a large (about 4 cm×5 cm), sensor hand-painted on textile, identical with one used in [5], is shown in Fig. 3 (see also [5]). Notice that interdigital capacitive sensors with the electrodes printed or deposited on the plastic walls, or embedded in the walls are well suited for the application, while plane-parallel plate capacitors with elastomeric dielectrics, as proposed in several studies, are less suitable, because of their non-negligible thickness. Cost and adaptation to any shape of the support were also factors when we suggested the use of interdigital capacitors for wearables [5]. Pictures of such sensors painted on textile are shown in [5] and experimental results with them sensors are given in [5] and [6].

III. Basic Theory of the Flexible Sensors

In this section we present several approximations of the capacitance of the sensor and study the errors occurring under various circumstances, under these approximations. We are mainly interested in comb capacitive sensors on textiles or thin foils, as used in [5]. Wearable interdigital (comb) sensors pose specific problems because of the various deformations of the textile or film supporting or embedding them.

A. *Capacitance of the planar interdigital sensor– in-plane parallel electrodes* [21-29]

We assume that the sensor is an interdigital one, with the geometry as in Fig. 4(a). Its capacitance was calculated under various hypotheses and reported in papers as [18-26]. Several authors [19,20,23-25] have presented calculations for interdigital sensors with strips (electrodes) not in the same plane, which is of special interest for flexible sensors.

There are several approximate formula for the capacitance of the interdigital sensor, including the simple parallel plate approximation, the approximation obtained using Schwartz-Christofell conformal mapping without and with taking into account the fringe field approximations derived from finite element simulations, and semi-empirical approximations, based on matching a proposed formula with the measurement results [19,20,23-25].

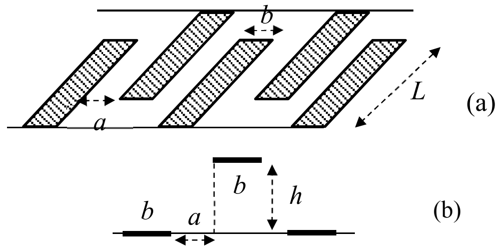

Figure 4. (a) Geometry of the interdigital in-plane sensor. (b) Out of plane sensor.

Much of the related work was devoted to MEMS technology, especially MEMS actuators and sensors, with some older contributions related to radio-frequency circuits. For planar structures with thick substrates, [22] proposed $C\ [pF] = ((\varepsilon_r + 1)/W) \cdot l \cdot [(N-3)A_1 + A_2]$, with $A_1 \approx 8.85 \cdot 10^{-12}\, b$, $A_2 \approx 9.9 \cdot 10^{-12} W$, where b [cm] is the width of the electrodes, N the number of electrodes, $N(a+b) = W$ is the overall width of the electrodes, see Fig. 4(a), l [cm] is the lengths of the digits. The approximation is valid for thicknesses of the substrate, t_h, much larger than the distance between digits (strip spacing), a, $t_h/a > 100$, which is not respected for planar capacitors on thin foils. The formula also assumes very small values of a, of the order of microns [22]. Bahl [21] (equ 7.7b) provides a more general and precise formula for the planar interdigital capacitance in terms of complete elliptic integral of the first kind, $K(.)$:

$$C\ [pF] = 10^{-3}\, \frac{\varepsilon_r}{18\pi} \cdot \frac{K(k)}{K'(k)} \cdot l \cdot (N-1) \qquad (1)$$

with $[l]$ is in μm, k is the elliptic modulus, $k = \tan^2 \frac{\pi c}{4d}$, $c = b/2$, $d = (a+b)/2$, and $k' = \sqrt{1-k^2}$. The ratio $\frac{K(k)}{K\prime(k)}$ (of the complete elliptic integral of first kind to its complement) is according to equ. (7.8 a,b) and (7.9) in [21],

$$\frac{K(k)}{K\prime(k)} = \begin{cases} \frac{1}{\pi} \cdot ln\left(2\,\frac{1+\sqrt{k}}{1-\sqrt{k}}\right) & for\ 0.707 \le k \le 1 \\ \pi / ln\left(2\,\frac{1+\sqrt{k\prime}}{1-\sqrt{k\prime}}\right) & for\ 0 \le k \le 0.707 \end{cases} . \quad (2)$$

(all the above from Bahl [21]; see also [5]).

B. *Capacitance of the planar interdigital sensor– out-of-plane parallel electrodes* [18-27]

According to [27] for a pair of successive fingers, the capacitance of a comb sensor with plan parallel but out of plane successive electrodes is, for a pair of successive electrodes, the capacitance is [27]

$$C \approx \frac{2\pi\varepsilon_0 L}{\pi^2 - \arctan^2 \frac{2h}{a+b}} \times \ln\left(1 + \frac{b}{a}\right) \qquad (3)$$

where the notations are as in Fig. 4(b). This formula will be extensively used in this study.

The formulas above are useful in case when the capacitor and its support remain perfectly planar, that is, when the planar support is stretching (or allows compression yet maintaining the planar form, which is rare) along directions in its plane. However, more important for wearable and flexible sensors is the case when the support of the sensor changes shape from planar to curve or folded. This case is dealt with subsequently.

C. Capacitance of the out-of-plane, tilted (non-parallel) electrodes

Numerous configurations of the successive electrodes may appear when the sensors bend following folds and smaller wrinkles of the skin or clothes during the movements of the human body parts. The specific configuration depends on the geometry of the skin or clothes folds, on the dimensions of the folds, and on the width of the electrodes, b, and spaces between them, a. When the radius of curvature of the fold is comparable with b, $b > a$, several cases of sensor folding may be produced, for example those in Fig. 5(a)-(e). These cases have to be dealt distinctly, because there is no one single formula for all of them.

For small curvature radius of the wrinkles compared with b, as in Fig. 5(a), examples of shapes assumed by the sensor are shown in Fig. 5(b), 5(c), where 5(c) is based on [24], and 5(e). These two cases differ by the way the axes of the electrodes (in transversal plane) intersect: in Fig. 5(b) and 5(e) the axes intersect outside the electrodes, while in Fig. 5(c) the axis of the tilted electrode intersects the horizontal electrode. Figures 5(d) and 5(f) are complementing, with geometrical details, Fig. 5(c) and 5(e) respectively.

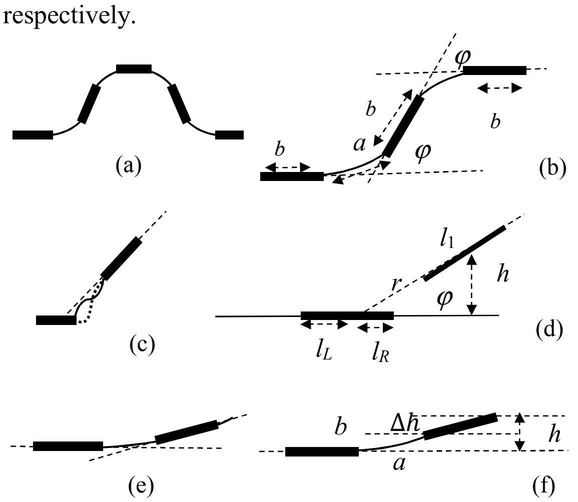

Figure 5. Non-parallel plate configurations, with the sensor seen in cross-section. Thick lines represent the electrodes. $l_R = \nu a$

For the tilted plate case depicted in Fig. 5(c) and (d), according to [24], [25] and [26], the capacitance is computed as the sum of the inner and outer capacitances of the facing plates, $C = C_{in} + C_{out}$. These capacitances, for the geometry in Fig. 5(d), are given by [24, 25] (equations 7-12 in [24], with simplified notations) and [26]; without the constant multiplier the expression is:

$$C/\varepsilon = \frac{K'(k_{Rin})}{K(k_{Rin})} + \frac{K'(k_{Rout})}{K(k_{Rout})} + \frac{K'(k_{Lin})}{K(k_{Lin})} + \frac{K'(k_{Lout})}{K(k_{Lout})} \quad (4)$$

where $K(\mathrm{k})$ is the complete elliptic integral of the first kind and, from [24, 25],

$$k_{Rin} = \sqrt{\frac{r^{\frac{\pi}{\varphi}}\left((r+l_1)^{\frac{\pi}{\varphi}}+l_R^{\frac{\pi}{\varphi}}\right)}{(r+l_1)^{\frac{\pi}{\varphi}}\left(r^{\frac{\pi}{\varphi}}+l_R^{\frac{\pi}{\varphi}}\right)}}, \quad (5)$$

$$k_{Rout} = \sqrt{\frac{r^{\frac{\pi}{2\pi-\varphi}}\left((r+l_1)^{\frac{\pi}{2\pi-\varphi}}+l_R^{\frac{\pi}{2\pi-\varphi}}\right)}{(r+l_1)^{\frac{\pi}{2\pi-\varphi}}\left(r^{\frac{\pi}{2\pi-\varphi}}+l_R^{\frac{\pi}{2\pi-\varphi}}\right)}}. \quad (6)$$

The value of k_{Lin} is obtained from k_{Rin} by replacing everywhere the exponent $\frac{\pi}{\varphi}$ by $\frac{\pi}{\pi-\varphi}$; the value of k_{Lout} is obtained from k_{Rout} by replacing everywhere the exponent $\frac{\pi}{2\pi-\varphi}$ by $\frac{\pi}{\pi+\varphi}$. When the electrodes have the same width, $l_1 = l_R + l_L$.

For the case in Fig. 5, in first approximation we consider, for small curvatures of the sensor in the regions without electrodes, $r \approx a$, $l_R = \nu a$, $l_L = b - \nu a$, $l_1 = b$, $\nu > 0$. Notice that in Fig. 5(c) only one electrode contributes to the height of the wrinkle (the simplest case to consider), but several electrodes and the corresponding inter-electrode spaces may be included in the increasing and decreasing sections of the wrinkle. Under these approximations, we derive

$$k_{Rin} \approx \sqrt{\frac{a^{\frac{\pi}{\varphi}}\left((a+b)^{\frac{\pi}{\varphi}}+(\nu a)^{\frac{\pi}{\varphi}}\right)}{(a+b)^{\frac{\pi}{\varphi}}\left(a^{\frac{\pi}{\varphi}}+(\nu a)^{\frac{\pi}{\varphi}}\right)}} = \sqrt{\frac{(a+b)^{\frac{\pi}{\varphi}}+(\nu a)^{\frac{\pi}{\varphi}}}{(a+b)^{\frac{\pi}{\varphi}}\left(1+(\nu)^{\frac{\pi}{\varphi}}\right)}} \quad (7)$$

and similarly, for k_{Rout}, k_{Lin}, k_{Lout}. In case $a \ll b$, as usually assumed, $a + b \approx b$ and , $a + b \gg \nu a$ and we can further approximate, using $(1 + x)^c = 1 + cx$, with $c = -1/2$,

$$k_{Rin} \approx \sqrt{\frac{1}{1+(\nu)^{\frac{\pi}{\varphi}}}} \approx 1 - \frac{1}{2}(\nu)^{\frac{\pi}{\varphi}}, \quad (8)$$

Because $\nu<1$ and $\varphi \ll \pi$, k_{Rin} is close to 1; this leads us to the use the approximation

$$\frac{K(k)}{K\prime(k)} = \frac{1}{\pi} \cdot ln\left(2\frac{1+\sqrt{k}}{1-\sqrt{k}}\right) \approx \frac{1}{\pi} \cdot ln\left(2\frac{1+\sqrt{k}}{1-\sqrt{k}}\right) \quad (9)$$

with the k from above; this introduces a new formula for computing soft capacitors in wearable and patch-type sensor. Notice that the case $\nu = 0$ is degenerate, with infinite ratio; it is why we impose $\nu > 0$.

The variation of the first term, $\frac{K'(k_{Rin})}{K(k_{Rin})}$, in the expression of the capacitance is graphed in Fig. 6. Various approximations are given in the literature for the elliptic integrals [28], [29], [30]. These approximations may be used to further refine the results in this section.

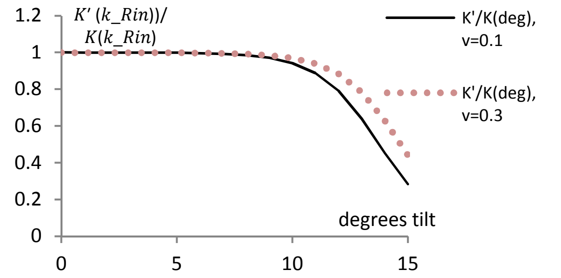

Figure 6. Variation of one of the terms in the tilted electrode capacitance (see text)

D. Case of snapping (plane switching) electrodes

One of the most simple shape changes when the sheet is compressed along its plane is by plane switching (snapping) of one or several digital electrodes. This may happen when the regions of the electrodes and (some of) the spaces between them are stiff, but the connecting regions between electrodes and spacing regions are soft. Such a configuration may make some of the electrodes snap into a different plane than the neighboring electrodes. Similar structures exhibiting this behavior are some side-folding security grilles and curtains. While such sensors have not been proposed previously, similar structures are known; therefore, we suggest that up-down snapping sensors could be a new design with advantages in applications where the sensor is compressed in a transversal (in-plane) direction.

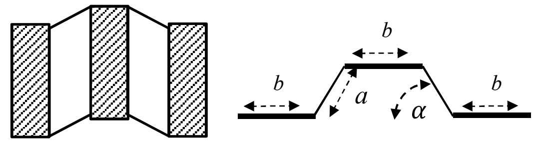

(a) (b)

Figure 7. Models of folding of the textile with the comb sensor, with electrodes preserving parallelism by plane-switching at compression.

The wrinkles formed by the contraction of the sensor may have the shape as in Fig. 7(a,b). In this case, the out-of-plane parallel electrodes case applies [18-26] and the formulas to use are those in [27].

IV. Sensitivities and Associated Nonlinearities of Deformed Interdigital Electrodes

A. Sensitivity of the in-plane electrodes to elongation

From the above formulas, the sensitivity to in-plane extension of the sensor, resulting in a transversal extension, i.e., in the increase of distance between the fingers, but assuming the fingers of constant width, is computed only for the realistic (thin substrates) formula based on elliptic integrals:

$$\frac{dC}{da} = 10^{-3}\,\frac{\varepsilon_r}{18\pi}\cdot l\cdot(N-1)\cdot\frac{d}{da}\left(\frac{K(k)}{K'(k)}\right). \quad (10)$$

Assuming the case $0.707 \leq k \leq 1$, with λ the constant in front of the derivative, we derive

$$\frac{\pi}{\lambda}\cdot\frac{dC}{da} = \frac{d}{da}\left(ln\left(2\frac{1+\sqrt{k}}{1-\sqrt{k}}\right)\right) \quad (11)$$

$$\frac{\pi}{\lambda}\cdot\frac{dC}{da} = \frac{1-\sqrt{\tan^2\frac{\pi c}{4d}}}{1+\sqrt{\tan^2\frac{\pi c}{4d}}}\,\frac{d}{da}\left(\frac{1+\sqrt{\tan^2\frac{\pi c}{4d}}}{1-\sqrt{\tan^2\frac{\pi c}{4d}}}\right) \quad (12)$$

Taking into account that $c = b/2$ is independent of a, only d depends on a and $\frac{d}{da}(d) = 1/2$. Using $c = b/2$, $d = (a+b)/2$, we derive

$$\tan^2\frac{\pi c}{4d} = \tan^2\frac{\pi b}{4(a+b)} < \tan^2\frac{\pi}{4} < 1, \quad (13)$$

$$\left(\tan^2\frac{\pi c}{4d}\right)' = 2\tan\frac{\pi c}{4d}\cdot\frac{\frac{\pi}{4}\frac{-1}{(a+b)^2}}{\cos^2\frac{\pi c}{4d}}. \quad (14)$$

When $a \ll b$, we derive after some algebra that the sensitivity is

$$\frac{\pi}{\lambda}\cdot\frac{dC}{da} \approx \frac{\pi}{4}\frac{-1}{b^2\left(1+\frac{a}{b}\right)^2}\left(1-\tan\frac{\pi}{4\left(1+\frac{a}{b}\right)}\right). \quad (15)$$

Therefore, the absolute sensitivity is greater when $\frac{a}{b} \to 0$ and b is small ($b \to 0$ in $\frac{-1}{(a+b)^2}$). We derive that the relative sensitivity is, for $0.707 \leq k \leq 1$,

$$\frac{1}{C}\frac{dC}{da} = \frac{1}{\frac{K(k)}{K'(k)}}\frac{d}{da}\left(\frac{K(k)}{K'(k)}\right) =$$

$$\frac{1}{\frac{1}{\pi}ln\left(2\frac{1+\sqrt{\tan^2\frac{\pi c}{4d}}}{1-\sqrt{\tan^2\frac{\pi c}{4d}}}\right)}\,\frac{1-\sqrt{\tan^2\frac{\pi c}{4d}}}{1+\sqrt{\tan^2\frac{\pi c}{4d}}}\cdot\frac{d}{da}\left(\frac{1+\sqrt{\tan^2\frac{\pi c}{4d}}}{1-\sqrt{\tan^2\frac{\pi c}{4d}}}\right) \quad (16)$$

Notice that, for longitudinal elongation, $C(L)$ has a linear expression, therefore the sensitivity along the direction of the fingers is constant and low. This allows making the sensor essentially sensitive along a single direction. With two orthogonal sensors, one can determine the direction of stretching.

B. Sensitivity of capacitors with out-of-plane successive electrodes, with plane switching

Assume that the folding is due to in-plane compression (in the sensor plane) and that this type of folding produces plane switching of the electrodes, such that the distance between the electrodes, a, essentially remains the same (a strong approximation). Then, for a pair of successive fingers, we derive the relative sensitivity of the capacitance to deformation

$$\frac{1}{C}\frac{dC}{dh} = \left(\pi^2 - \arctan^2\frac{2h}{a+b}\right)\frac{d}{dh}\left(\frac{1}{\pi^2-\arctan^2\frac{2h}{a+b}}\right) \quad (17)$$

Denoting $\frac{2h}{a+b} = u$ one obtains $\frac{d}{dh}\left(-\arctan\ u(h)\right) = \frac{u'}{1+u^2}$, $u' = \frac{2}{a+b}$, therefore

$$\frac{1}{C}\frac{dC}{dh} = \frac{4}{a+b}\,\frac{\arctan u}{\pi^2-\arctan^2 u}\,\frac{1}{1+u^2}. \quad (18)$$

Graphs of the sensitivities $\frac{1}{C}\frac{dC}{dh}$ for several combinations of the ratios of a, b, where for $b = 0.001$, are shown in Fig. 8. Notice that the graphs in Fig. 8 are of interest only for heights less than a, whose maximal value is $b = 0.001$. The graphs in

Fig. 9 are shown only for values of the height that make sense for the chosen parameters.

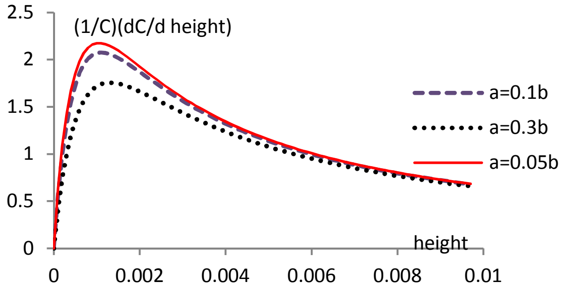

Figure 8. Theoretical characteristic of the sensitivity of out-of-plane interdigital flexible sensor, $S_h = \frac{1}{C} \cdot \frac{dC}{dh}$, for an infinitely stretchable support. Results for b=0.001.

The sensor cannot be considered linear, except for small intervals. A quadratic approximation works well for all cases of ratios $0.3 \leq \frac{a}{b} \leq 1$, for the ranges where the capacitor support does not stretches, that is, for $h \leq a$, For example, for $b = 1\ mm, a = 0.3\ mm$, $h \leq a$, the approximation $S_h = -4 \cdot 10^6 h^2 + 4544.8h + 0.0063$ has the coefficient of determination $R^2 = 0.9998$ for $h \in [0{,}0.1]\ mm$, and for $b = 1\ mm, a = 0.3\ mm, h \leq a$, a good approximation is $S_h = -2 \cdot 10^6 h^2 + 3258h + 0.0134$ with $R^2 = 0.999$ for $h \in [0{,}0.3]\ mm$.

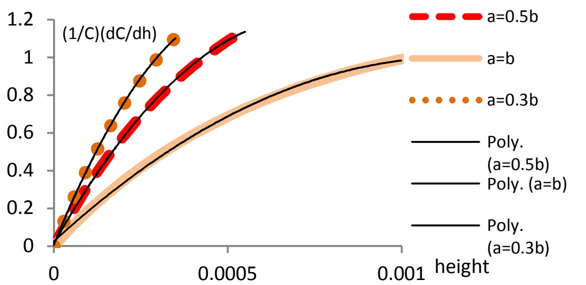

Figure 9. Realistic zone of the out-of-plane interdigital sensor operation (no stretch). $b = 1\ mm, h \leq a$.

The approximation for $a = b = 0.001$ ($S_h = -733015h^2 + 1691.2h + 0.0249$, $R^2 = 0.9988$) is also almost indistinguishable on the graph of the S_h curve (Fig. 8 and 9).

C. Sensitivity of capacitors with out of plane successive electrodes, with plane tilting

For tilting electrodes, according to Section III-C), the sensitivity was computed for one of the terms in [24], namely for $C_1/\varepsilon = \frac{K'(k_{Rin})}{K(k_{Rin})}$. The values obtained for $\nu = 0.1$ and $\nu = 0.3$ are shown in Fig. 10.

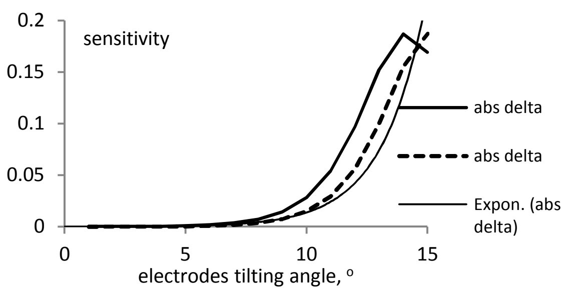

Figure 10. The exponential increase in sensitivity of the capacitive sensor with tilting electrodes. Dotted line for $\nu = 0.3$. Thick line $\nu = 0.1$. See legend to Fig. 5 and text for ν's definition.

Notice that the sensitivity grows exponentially for small angles, making such sensors insensitive to small deformations that only tilt the electrodes under the described conditions (for angles less than about 7-10°). Also notice for small values of ν (ν =0.1) that the interval of monotonic and significant variation of the capacitance is from about 5° to 15°.

V. Discussion and Conclusions

We thoroughly analyzed the theoretical properties of large, flexible interdigital capacitive sensors on the surface of foils, textiles, and other deformable materials. Such sensors can find applications in monitoring the inflation state of collapsible enclosures, the smoothness of the surface of textiles such as textile industrial covers, or of textiles of medical use such as large surface wound dressings and bed covers.

The various types of transversal deformations of the sensors have been discussed for one pair of electrodes. Notice that the folding may occur only on a section of the interdigital capacitor, representing γ% of the surface of the capacitor. Then, the factor γ multiplies the effects described in Section IV.

The large number of mechanisms and patterns of deformation of the flexible capacitive sensors used as patches on the skin, placed on or embedded in textiles, or placed on or embedded in flexible foils makes the analysis of their behavior very tedious. In addition, the results of the analysis remain limited to the specific combination of materials, dimensions, deformation amplitudes, and support (skin, foil, or textile) analyzed. The variety of geometries and support-sensor interactions and assumed shapes produce very different nonlinear expressions for the sensitivity of the sensor to local deformations in a normal direction to the electrodes. Also because of the variety of involved processes, the flexible capacitive interdigital sensors exhibit a set of nonlinearities when deformed in a normal direction to the electrodes.

We derive that interdigital capacitive sensors have a good enough operation (linearity and monotony) only for small enough tilting angle of successive electrodes (from a few degrees to less than 10°) and for small out-of-plane displacements of the electrodes compared with the electrode widths. A practical conclusion is that the width of the electrodes and their inter-space should be commensurate with the thickness of the textile or foil on which they are placed. When this condition is satisfied, because the folding of the substrate is typically produced with curvature radii much larger than the thickness of the substrate, the tilting of the successive electrodes and their out of plane displacement is small. As a consequence, the induced change in the capacitance is reasonably small and monotonic with the change in geometry.

For some applications, such as the sensing of the inflation state of a collapsible enclosure, only a specified value of the capacitance matters (the value when the inflation is complete). Using such an interdigital sensor on the surface of an inflatable enclosure and coupling the sensor to a capacitance-to-number or voltage circuit would allow the easy detection of the full inflation state, by the capacitance attaining a specified value. This could replace the use of pressure sensors in the application described in our parallel paper in this conference.

The analytical treatment in this study adds to the theoretical contributions of Eidenberger and Zagar [23], of Xiang [24], [25], and of Hu et al. [27]. The analysis performed helps in understanding the operation of these types of sensors; it may also help in choosing methodically the parameters of the flexible capacitive interdigital sensors, including width of the electrodes, distance between them, rigidity of the electrodes and the support, and overall dimensions of the sensor, in relation with the application dealt with.

Acknowledgments. This work was not supported by any grant or institution / company.

Note. This paper relies on, continues, and complements the paper [5] in the references.

Authors' contributions. MT proposed the use of the sensors from [5] in the context of the new applications described in this paper and suggested a detailed analysis of their behavior and accuracy. He contributed to sections I, II and V and to the reference list. HNT contributed to all sections and wrote sections III and IV who bears full responsibility for these sections.

Conflict of interest. Patents pending. MT declares an interest in improving the SurgiBox product produced by SurgiBox Inc., USA.

REFERENCES

[1] T. Grosse-Puppendahl, C Holz, G Cohn, "Finding common ground: A survey of capacitive sensing in human-computer interaction." Proceedings of the CHI 2017, May 6–11, 2017, Denver, CO, USA, pp. 3293-3316, dl.acm.org, https://dl.acm.org/doi/pdf/10.1145/3025453.3025808.

[2] J. Ferri, L. Llinares, J. Moreno, V. Lidón-Roger & E. Garcia-Breijo, (2020) "An investigation into the fabrication parameters of screen-printed capacitive sensors on e-textiles", Textile Research J. doi: 10.1177/0040517519901016.

[3] H. Djelouat, X.J. Zhai, M. Disi, A. Amira, F. Bensaali, "System-on-chip solution for patients biometric: A compressive sensing-based approach." IEEE Sens. J. 2018, vol. 18, pp. 9629–9639.

[4] M. Stoppa and A. Chiolerio, "Wearable electronics and smart textiles." Sensors 2014, vol. 14, 7, pp. 11957-11992.

[5] H.N. Teodorescu, "Textile-, conductive paint-based wearable devices for physical activity monitoring." Proc. 4th IEEE Int. Conf. E-Health and Bioengineering (EHB), Iasi, Romania Nov 21-23, 2013.

[6] M. Hagan, H.N. Teodorescu, "intelligent clothes with a network of painted sensors." Proc. 4th IEEE Int. Conf. on E-Health and Bioengineering (EHB), Iasi, Nov 21-23, 2013.

[7] A. Barleanu, M. Hagan, O. Geman, I. Chiuchisan, "Wearable ballistocardiography system for heartbeat detection," 2016 Int. Conf. Exposition Electrical and Power Engineering (EPE), Iasi, 2016, pp. 294-298.

[8] A. Brezulianu et al., "IoT based heart activity monitoring using inductive sensors." Sensors, Vol. 19, 15, 10.3390/s19153284.

[9] H.N. Teodorescu, V. Cojocaru, "Biomimetic chaotic sensors for water salinity measurements and conductive titrimetry". Proc. Third Int. Conf. on Emerging Security Technologies (EST), Sept 5–7, 2012, Stoica, A. et al., Eds., Lisbon, 2012, pp. 182-185.

[10] V.P. Cojocaru, "Characterization of interdigital electrode sensors." Surf. Engin. Appl. Electrochem. Vol. 55, pp. 225–231 (2019). https://doi.org/10.3103/S1068375519020078

[11] W.-C. Chuang, H.-L. Lee, P.-Z. Chang, Y.-C. Hu, "Review on the modeling of electrostatic MEMS." Sensors 2010, vol. 10, 6149-6171; doi:10.3390/s100606149

[12] T. Kaya, B. Shiari, K. Petsch, D. Yates, "Design of a MEMS capacitive comb-drive accelerometer." COMSOL Conf., 2011, Boston, www.comsol.com/paper/download/100777/kaya_paper.pdf.

[13] L.-S. Zheng, M.S.-C. Lu, "A large-displacement CMOS-micromachined thermal actuator with capacitive position sensing." 2005 IEEE pp. 89-92, http://citeseerx.ist.psu.edu/viewdoc/download?doi=10.1.1.118.3589&rep=rep1&type=pdf.

[14] D.L. Teodorescu et al., Patent application WO 2018/014003A1, Ultraportable System for Intraoperative Isolative and Regulation of Surgical Site Environments.

[15] D.L. Teodorescu, D. Nagle, J. Gómez-Márquez, et al., UNESCO-EPFL Tech4Dev Conf. 2016 http://cooperation.epfl.ch/files/content/sites/cooperation/files/1171-Teodorescu-SE07-MED_Full%20Paper.pdf.

[16] *** Spotlight on: SurgiBox, StartHub's Startup to Watch for July 2018. https://d-lab.mit.edu/news-blog/news/spotlight-surgibox-starthubs-startup-watch-july-2018.

[17] D. Teodorescu, M. Teodorescu, S. Okajima, SurgiBox. In Beazley Designs of the Year 2018, by The Design Museum, London, U.K., 2018, ISBN 978187200541-6, pp. 192-193.

[18] E. Gallagher, W. Moussa, "A Study of the effect of the fringe fields on the electrostatic force in vertical comb drives." Sensors 2014, vol. 14, pp. 20149-20164.

[19] L. Gao and D. Zhao, "The fringing capacitance of an inclined plate capacitor." Fundamental J. Math. Physics, Vol. 2, Issue 1, 2012, pp. 11-17.

[20] J.-M. Bueno-Barrachina, C.-S. Cañas-Peñuelas, S. Catalan-Izquierdo, F. Cavallé-Sesé, "Capacitance evaluation on perpendicular plate capacitors by means of finite element analysis". Int. Conf. Renewable Energies and Power Quality (ICREPQ'09), Valencia (Spain), 15-17th Apr, 2009. http://www.icrepq.com/ICREPQ'09/452-barrachina.pdf .

[21] I.J. Bahl, Lumped elements for RF and microwave circuits. Artech House, Boston, London, 2003, Ch. 7, p. 229.

[22] I. Thayne, K. Elgaid, G. Ternent, "Devices and fabrication technology." Chapter 2, in I.D. Robertson, S. Lucyszyn (Eds.), RFIC and MMIC Design and Technology. IET, 2001, London, UK pp. 40-41.

[23] N. Eidenberger, B.G. Zagar, "Capacitive sensor design utilizing conformal mapping methods." Int. J. Smart Sensing & Intelligent Systems, Vol. 5, No. 1, Mar 2012, 36-56.

[24] Y. Xiang, "Further study on electrostatic capacitance of an inclined plate capacitor." J. of Electrostatics, Vol. 66, Issues 7–8, Jul 2008, pp. 366–368.

[25] Y. Xiang, "The electrostatic capacitance of an inclined plate," J. of Electrostatics, Vol. 64, 1, 2006, 29–34.

[26] J.M. Bueno-Barrachina, C.S. Cañas-Peñuelas and S. Catalan-Izquierdo, "Capacitance evaluation on non-parallel thick-plate capacitors by means of finite element analysis." J. Energy and Power Engineering, vol. 5 (2011) 373-378.

[27] C. Hu, D. Zheng, S. Fan, G. Zhanshe, "Theoretical and experimental research on the in□plane comb□shaped capacitor for MEMS Coriolis mass flow sensor." Microsyst Technol, DOI 10.1007/s00542-015-2441-7, Online March 2015.

[28] Y.L. Luke, "Approximations for Elliptic Integrals." Math. Comp. 22 (1968), pp. 627-634, DOI: https://doi.org/10.1090/S0025-5718-1968-0226825-3.

[29] Yudell L. Luke, "Further approximations for elliptic integrals." Math. Comp. vol. 24 (1970), pp. 191-198. DOI: https://doi.org/10.1090/S0025-5718-1970-0258243-5.

[30] E.W. Weisstein, "Complete elliptic integral of the first kind." MathWorld--A Wolfram Web Resource. https://mathworld.wolfram.com/CompleteEllipticIntegraloftheFirstKind.html.